Hindawi Publishing Corporation
International Journal of Antennas and Propagation
Volume 2015, Article ID 563737, 9 pages
http://dx.doi.org/10.1155/2015/563737

Research Article

Asynchronous Two-Way Relaying Networks Using Distributed Differential Space-Time Coding

Minjie Qian, Yanliang Jin, Zhuo Wu, and Tao Wang

Key Laboratory of Specialty Fiber Optics and Optical Access Networks, Shanghai University, Shanghai 200072, China

Correspondence should be addressed to Zhuo Wu; zwu@shu.edu.cn

Received 25 June 2014; Revised 19 August 2014; Accepted 27 August 2014

Academic Editor: Lingyang Song

A signal detection scheme is proposed for two-way relaying network (TWRN) using distributed differential space-time coding (DDSTC) under imperfect synchronization. Unlike most of existing work, which assumed perfect synchronization and channel state information (CSI) at all nodes, a more realistic scenario is investigated here by considering the signals transmitted from the two source nodes arriving at the relay not exactly at the same time due to the distributed nature of the nodes, and no CSI is available at any node. The proposed signal detection scheme is then demonstrated to remove the imperfect synchronization effect significantly through simulation results. Furthermore, pairwise error probability (PEP) of the asynchronous TWRN is analyzed and derived for both source nodes. Based on the simplified PEP expression, an optimum power allocation (OPA) scheme is then determined to further improve the whole system performance, when neither the source nor the relay has any knowledge of the CSI.

1. Introduction

Cooperative communications have attracted much attention nowadays, by allowing nodes in the network to cooperate and form a virtual antenna array [1, 2]. Compared with one-way relaying, two-way relaying networks (TWRNs) [3] have the advantage of high spectral efficiency, where two source nodes exchange information via the help of the relay nodes located between them. Recently, distributed space-time coding (DSTC) for TWRNs was extensively investigated [4–6] due to the diversity and multiplexing gain of multiple-input and multiple-output (MIMO) technology. Most of the existing studies on DSTC consider coherent detection by assuming that the channel state information (CSI) is known at the receiver. However, in fast-fading scenario, accurate CSI is hard to acquire, and training symbols required for channel estimation will decrease the spectrum efficiency and increase computation complexity, especially when there are multiple relays in wireless networks. Therefore, differential modulation has been considered to address this problem since it does not require the knowledge of CSI at either the transmitter or the receiver [7, 8].

Similar to the coherent detection scenario [9, 10], several protocols have been proposed for TWRNs using differential detection. One of the most commonly used protocols is the amplify-and-forward (AF) scheme [11, 12]. In this scheme, both source nodes transmit information to the relay node at the same time, the relay then amplifies the received superimposed signal and broadcasts to both sources. For multiple relay nodes, space-time coding is used before amplifying the signals. This AF based bidirectional relaying is also referred to as analog network coding (ANC), which is very useful in wireless networks since the wireless channel acts as a natural fulfillment of network coding by superimposing the wireless signals over the air. In [11], distributed differential space-time coding by AF was applied to TWRNs for the first time. However, the correctness of the currently detected symbol significantly affects the decoding of next symbols, resulting in severe error propagation. To solve this problem, Huo et al. [12] presented a differential space-time coding with distributed ANC (DDSTC-ANC) scheme for TWRNs with multiple relays. The DDSTC-ANC scheme has been proved to achieve the same diversity order as the coherent detection scheme, but the performance of which is 3 dB away compared

with that of the coherent detection due to the differential modulation.

So far, almost all work on DDSTC with TWRNs has assumed that the transmission is perfectly synchronized by assuming that the relay nodes receive the signals from both source nodes at the same time, which can be difficult to achieve in practical systems due to the distributed nature of the nodes, and the channels may become dispersive with imperfect synchronization even under flat fading [13–16]. In [15], a signal detection scheme for differential bidirectional relaying with ANC under imperfect synchronization was put forward, but it only considers a single relay node. In [16], the authors proposed a simple detection scheme for distributed space-time block coding under imperfect synchronization for TWRNs. However, perfect CSI is required at all nodes. To the best of our knowledge, little has been reported for TWRNs with multiple relays using DSTC under imperfect synchronization, when neither the sources nor the relays have any knowledge of the CSI.

Therefore, a differential signal detection scheme for asynchronous TWRNs with multiple relays using DDSTC is proposed in this paper. Due to imperfect synchronization, the symbols that relays broadcast back to sources are not symmetrical, signal detection will not be the same at the two sources, which will be described in detail thereafter. Due to the importance of resource allocation for the TWRN system [17, 18], the performance of the proposed detection schemes is analyzed and PEP for both sides is derived. Moreover, an optimum power allocation (OPA) scheme is presented to further improve the system performance, based on the simplified PEP expression.

The rest of this paper is organized as follows. Section 2 introduces the system model. In Section 3, the detection schemes of the different sides are proposed, respectively, by two subsections. Section 4 presents the performance analysis and OPA for the system. The simulation results and corresponding conclusions are provided in Section 5. Section 6 summarizes the paper.

Notation. Throughout this paper, capital and boldface lowercase letters denote matrices and vectors, respectively. $(\cdot)^*$, $(\cdot)^T$, $(\cdot)^H$, and $(\cdot)^{-1}$ stand for complex conjugate, transpose, conjugate transpose, and inverse, respectively, for both matrix and vector. $\mathbb{E}\{\cdot\}$ denotes the expectation. diag $\{x_1, x_2\}$ represents 2×2 matrix whose ith diagonal entry is x_i.

2. System Model

A TWRN with two source nodes and two relay nodes is considered in this paper, all equipped with a single antenna and working in the half-duplex mode. The source nodes, S_1 and S_2, exchange information through relay nodes R_1 and R_2, using two phases, the multiple access (MA) phase and the broadcast (BC) phase, as shown in Figure 1. In the MA phase, both sources transmit signals to R_1 and R_2 simultaneously, while in the BC phase, the relays broadcast the amplified superimposed signal back to the source nodes. Let f_i and g_i $(i = 1, 2)$ denote the fading coefficients of the channels $S_1 - R_i$ and $S_2 - R_i$, respectively. In the MA phase, both relays

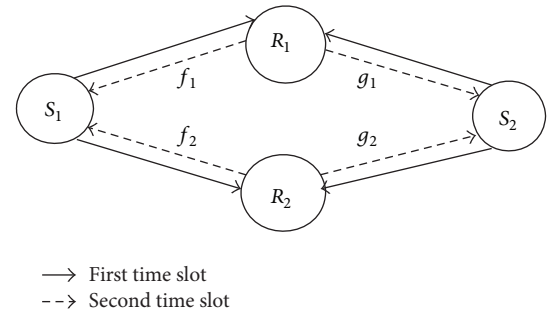

Figure 1: Transmission model of DTWRN.

receive a superposition of the signals transmitted from S_1 and S_2. The number of symbols in a distributed differential space-time coding block is normally assumed to be equal to the number of relay nodes. Since two relay nodes are considered in this TWRN, the signals transmitted from S_1 and S_2 can be represented as two-dimensional vectors $\mathbf{s}_j(t) = [s_{j1}(t) \;\; s_{j2}(t)]^T$ $(j = 1, 2)$, normalized as $E\{\mathbf{s}_j(t)\mathbf{s}_j(t)^H\} = \mathbf{I}$. Considering that $\mathbf{s}_1(t)$ and $\mathbf{s}_2(t)$ are imperfectly synchronized during the first phase, therefore they arrive at the relay nodes at different time with a relative time delay. In the distributed TWRNs, there are two nodes in the relay, the relative relay time of $\mathbf{s}_1(t)$ and $\mathbf{s}_2(t)$ at two relay nodes are different, and they are assumed as τ_1 and τ_2 corresponding to nodes R_1 and R_2, respectively. Since the effort of synchronization is always required, τ_1 and τ_2 are assumed no greater than the symbol period T. Such a relative time delay will still cause "intersymbol interference (ISI)" from neighboring symbols at the receiver. Without loss of generality, we assume that the signal from S_1 is perfectly synchronized to R_1 and R_2. The received signals at relay node R_i can then be expressed as

$$\begin{aligned}\mathbf{r}_i(t) = {} & \sqrt{P_1} f_i(t)\,\mathbf{s}_1(t) + \sqrt{P_2}\sqrt{1-\alpha_i^2}\, g_i(t)\,\mathbf{s}_2(t) \\ & + \sqrt{P_2}\alpha_i g_i(t-1)\,\mathbf{s}_2(t-1) + \mathbf{v}_i(t), \quad i = 1, 2,\end{aligned} \tag{1}$$

where P_1 and P_2 are the transmitted power of S_1 and S_2. $\mathbf{v}_i(t) = [v_{i1}(t) \;\; v_{i2}(t)]^T$ represents the noise in the MA phase, which follows a zero-mean white Gaussian distribution, that is, $\mathbf{v}_i(t) \sim \mathcal{CN}(0, N_0\mathbf{I})$. α_i stands for the imperfect coefficient of channel fading between S_2 and R_i, which reflects the effect of timing delay τ_i. Normally, we have $\alpha_i = 0$ for $\tau_i = 0$, which means the synchronization situation, and $\alpha_i = \sqrt{1/2}$ ($\alpha_i = \sqrt{1-\alpha_i^2}$) for $\tau_i = 0.5T$, which means the power of delay signal is equal to that of current signal. The fading coefficients $f_i(t)$ and $g_i(t)$, denoting the Rayleigh channel fading from source S_1 to Relay R_i and source S_2 to Relay R_i, that is, $f_i(t) \sim \mathcal{CN}(0, \sigma_{f_i}^2)$ and $g_i(t) \sim \mathcal{CN}(0, \sigma_{g_i}^2)$, are assumed to be constant over one frame and change independently from one frame to another for simplicity [15, 17, 18]. So, let $f_i(t) = f_i$, $g_i(t) = g_i$, and $\mathbf{r}_i(t)$ can be expressed as

$$\begin{aligned}\mathbf{r}_i(t) = {} & \sqrt{P_1} f_i \mathbf{s}_1(t) + \sqrt{P_2}\sqrt{1-\alpha_i^2}\, g_i \mathbf{s}_2(t) \\ & + \sqrt{P_2}\alpha_i g_i \mathbf{s}_2(t-1) + \mathbf{v}_i(t), \quad i = 1, 2.\end{aligned} \tag{2}$$

Since differential modulation is considered in this paper, a 2×2 unitary matrix $U(t)$ is used to encode the signal at nodes S_1 and S_2. At time t, it is encoded as $\mathbf{s}_j(t) = U_j(t)\mathbf{s}_j(t-1)$ $(j = 1, 2)$, where $\mathbf{s}_j(t-1)$ is the signal transmitted by S_i at time $t-1$. For space-time coding, a block is often constructed for transmission [10], which satisfies

$$\begin{aligned} A_k U_j(t) &= U_j(t) A_k, \quad \text{if } B_k = \mathbf{0}, \\ B_k U_j^*(t) &= U_j(t) B_k, \quad \text{if } A_k = \mathbf{0}, \end{aligned} \tag{3}$$

where A_k and B_k are two 2×2 complex matrices. For simplicity, it is designed that either A_k is unitary, $B_k = \mathbf{0}$ (case I), or B_k is unitary, $A_k = \mathbf{0}$ (case II).

In the BC phase, the ith relay node R_i utilizes $\mathbf{r}_i(t)$ to generate a symbol vector $\mathbf{x}_i(t)$ to satisfy the space-time coding scheme, which is a linear combination of $\mathbf{r}_i(t)$ and its conjugate [12, 19]. Hence, $A_1 = \left[\begin{smallmatrix} 1 & 0 \\ 0 & 1 \end{smallmatrix}\right]$, $B_2 = \left[\begin{smallmatrix} 0 & 1 \\ -1 & 0 \end{smallmatrix}\right]$. Considering amplify-and-forward (AF) protocol in the relay nodes, the transmitted signal at the ith relay can be represented as

$$\mathbf{x}_i(t) = \beta_i(t)\left(A_i \mathbf{r}_i(t) + B_i \mathbf{r}_i(t)^*\right), \tag{4}$$

where $\beta_i(t)$ is the scaling factor at R_i and specially given by

$$\begin{aligned} \beta_i(t) &= \sqrt{\frac{P_{R_i}}{\sigma_{f_i}^2 P_1 + \left(1-\alpha_i^2\right)\sigma_{g_i}^2 P_2 + \alpha_i^2 \sigma_{g_i}^2 P_2 + N_0}} \\ &= \sqrt{\frac{P_{R_i}}{\sigma_{f_i}^2 P_1 + \sigma_{g_i}^2 P_2 + N_0}}, \end{aligned} \tag{5}$$

where P_{R_i} is the transmitted power of R_i and it is assumed that $P_{R_i} = P_R$, so we have $\beta_i(t) = \beta$ (constant). Then, the relay nodes R_i broadcast the coded symbol vector $\mathbf{x}_i(t)$. The signals received at two source nodes are expressed as follows, respectively. At node S_1,

$$\begin{aligned} \mathbf{y}_1(t) &= \beta f_1 A_1 \mathbf{r}_1(t) + \beta f_2 B_2 \mathbf{r}_2^*(t) + \mathbf{w}_1(t) \\ &= \sqrt{P_1}\beta S_1(t)\begin{bmatrix} f_1^2 \\ f_2 f_2^* \end{bmatrix} + \sqrt{P_2}\beta S_2(t)\begin{bmatrix} \sqrt{1-\alpha_1^2} f_1 g_1 \\ \sqrt{1-\alpha_2^2} f_2 g_2^* \end{bmatrix} \\ &\quad + \sqrt{P_2}\beta S_2(t-1)\begin{bmatrix} \alpha_1 f_1 g_1 \\ \alpha_2 f_2 g_2^* \end{bmatrix} + \beta\begin{bmatrix} f_1 v_{11} & -f_2 v_{22}^* \\ f_1 v_{12} & f_2 v_{21}^* \end{bmatrix} \\ &\quad + \begin{bmatrix} w_{11}(t) \\ w_{12}(t) \end{bmatrix}, \end{aligned} \tag{6}$$

where $\mathbf{w}_i(t) = \left[w_{i1}(t) \;\; w_{i2}(t)\right]^T$ $(i = 1, 2)$ denotes the additive white Gaussian noise (AWGN) at S_1. $S_j(\tau)$ $(\tau = t, t-1)$ is the space-time coding block which satisfies (7), and it is also a linear construction of $s_j(\tau)$ and its conjugate [20]

$$S_j(\tau) = \left(A_1 \mathbf{s}_j(\tau), \; B_2 \mathbf{s}_j^*(\tau)\right) = \begin{bmatrix} s_{j1}(\tau) & -s_{j2}^*(\tau) \\ s_{j2}(\tau) & s_{j1}^*(\tau) \end{bmatrix}. \tag{7}$$

Besides, $S_j(t)$ is in the differential modulation with $S_j(t)$ as follows:

$$\begin{aligned} S_j(t) &= \left(A_1 \mathbf{s}_j(t), \; B_2 \mathbf{s}_j^*(t)\right) \\ &= \left(A_1 U_j(t) s_j(t-1), \; B_2 U_j^* s_j^*(t-1)\right) \\ &= \left(U_j(t) A_1 s_j(t-1), \; U_j(t) B_2 s_j^*(t-1)\right) \\ &= U_j(t) \cdot S_j(t-1). \end{aligned} \tag{8}$$

Let $\mathbf{h}_{11}(t) = \beta\left[\begin{smallmatrix} f_1^2 \\ f_2 f_2^* \end{smallmatrix}\right]$, $\mathbf{h}_{12}(t) = \beta\left[\begin{smallmatrix} \sqrt{1-\alpha_1^2} f_1 g_1 \\ \sqrt{1-\alpha_2^2} f_2 g_2^* \end{smallmatrix}\right]$, $\mathbf{h}_{13}(t) = \beta\left[\begin{smallmatrix} \alpha_1 f_1 g_1 \\ \alpha_2 f_2 g_2^* \end{smallmatrix}\right]$, and $\mathbf{n}_1(t) = \beta\left[\begin{smallmatrix} f_1 v_{11} & -f_2 v_{22}^* \\ f_1 v_{12} & f_2 v_{21}^* \end{smallmatrix}\right] + \left[\begin{smallmatrix} w_{11}(t) \\ w_{12}(t) \end{smallmatrix}\right]$; then $\mathbf{y}_1(t)$ can be abbreviated as

$$\begin{aligned} \mathbf{y}_1(t) &= \sqrt{P_1} S_1(t) \mathbf{h}_{11}(t) + \sqrt{P_2} S_2(t) \mathbf{h}_{12}(t) \\ &\quad + \sqrt{P_2} S_2(t-1) \mathbf{h}_{13}(t) + \mathbf{n}_1(t). \end{aligned} \tag{9}$$

It is easy to prove that $E\{\mathbf{n}_1(t)\mathbf{n}_1(t)^H\} = \sigma_{\mathbf{n}_1}^2(t)\mathbf{I}$, and $\sigma_{\mathbf{n}_1}^2(t) = \left(\sum_{i=1}^2 |\beta|^2 |f_i|^2 + 1\right) N_0$. Similarly, at node S_2,

$$\begin{aligned} \mathbf{y}_2(t) &= \beta g_1 A_1 \mathbf{r}_1(t) + \beta g_2 B_2 \mathbf{r}_2^*(t) + \mathbf{w}_2(t) \\ &= \sqrt{P_1} S_1(t) \mathbf{h}_{21}(t) + \sqrt{P_2} S_2(t) \mathbf{h}_{22}(t) \\ &\quad + \sqrt{P_2} S_2(t-1) \mathbf{h}_{23}(t) + \mathbf{n}_2(t), \end{aligned} \tag{10}$$

where $\mathbf{h}_{21}(t) = \beta\left[\begin{smallmatrix} g_1 f_1 \\ g_2 f_2^* \end{smallmatrix}\right]$, $\mathbf{h}_{22}(t) = \beta\left[\begin{smallmatrix} \sqrt{1-\alpha_1^2} g_1^2 \\ \sqrt{1-\alpha_2^2} g_2 g_2^* \end{smallmatrix}\right]$, $\mathbf{h}_{23}(t) = \beta\left[\begin{smallmatrix} \alpha_1 g_1^2 \\ \alpha_2 g_2 g_2^* \end{smallmatrix}\right]$, $\mathbf{n}_2(t) = \beta\left[\begin{smallmatrix} g_1 v_{11} & -g_2 v_{22}^* \\ g_1 v_{12} & g_2 v_{21}^* \end{smallmatrix}\right] + \left[\begin{smallmatrix} w_{21}(t) \\ w_{22}(t) \end{smallmatrix}\right]$, and $\mathbf{n}_2$ has the same property as $\mathbf{n}_1$; that is, $\sigma_{\mathbf{n}_2}^2(t) = \left(\sum_{i=1}^2 |\beta|^2 |g_i|^2 + 1\right) N_0$.

For the first block, a known vector can be transmitted to both source nodes for differential modulation which satisfies $\{\mathbf{s}_j(t)^H \mathbf{s}_j(t)\} = 2$ $(j = 1, 2)$, for example, $\left[1 \;\; 1\right]^T$. Here, let $\mathbf{s}_1(0) = \left[1 \;\; 1\right]^T$, $\mathbf{s}_2(0) = \left[1 \;\; 1\right]^T$ as initial state; then $S_1(0) = \left[\begin{smallmatrix} 1 & -1 \\ 1 & 1 \end{smallmatrix}\right]$, $S_2(0) = \left[\begin{smallmatrix} 1 & -1 \\ 1 & 1 \end{smallmatrix}\right]$.

3. Signal Detection

Due to the imperfect synchronization, detection methods at the two source nodes are not the same. They are proposed and presented as follows, respectively.

3.1. Detection at Node S_1

Theorem 1. *If the relay matrices have the property:* $\mathrm{tr}\{O_i O_j^H\} = 2$ *for* $i = j$, $\mathrm{tr}\{O_i O_j^H\} = 0$ *for* $i \neq j$ *(where* O_j *stands for* A_j *or* B_j*) [12], it can be elicited that*

$$\mathbb{E}\left\{S_1(t)^H \mathbf{y}_1(t)\right\} = 2\sqrt{P_1}\mathbf{h}_{11}(t). \tag{11}$$

So, $\widetilde{\mathbf{h}}_{11}(t)$ *can be approximated as*

$$\widetilde{\mathbf{h}}_{11}(t) = \frac{1}{2L}\frac{1}{\sqrt{P_1}}\sum_{l=1}^{L} S_1(t-l)^H \mathbf{y}_1(t-l), \tag{12}$$

where L is the frame length. Then let

$$\begin{aligned}\tilde{\mathbf{y}}_1(t) &= \mathbf{y}_1(t) - \sqrt{P_1}S_1(t)\cdot\tilde{\mathbf{h}}_{11}(t)\\ &= \sqrt{P_2}S_2(t)\,\mathbf{h}_{12}(t) + \sqrt{P_2}S_2(t-1)\,\mathbf{h}_{13}(t) + \mathbf{n}_1(t).\end{aligned} \tag{13}$$

If detection of $\mathbf{s}_2(t)$ is in the same way as in the perfect synchronization case, that is, ignoring ISI $\sqrt{P_2}S_2(t-1)\mathbf{h}_{13}(t)$, there will be a severe error floor, which is the same at node S_2. To eliminate the error floor caused by imperfect synchronization, a detection scheme is proposed to remove the ISI as much as possible. When $t = 1$, the initial value is $\mathbf{h}_{13}(0) = 0$, $S_2(-1) = 0$; hence we have

$$\mathbf{y}_1(0) = \sqrt{P_1}S_1(0)\,\mathbf{h}_{11}(0) + \sqrt{P_1}S_2(0)\,\mathbf{h}_{12}(0) + \mathbf{n}_1(0). \tag{14}$$

Then $\tilde{\mathbf{y}}_1(0)$, $\tilde{\mathbf{y}}_1(1)$ can be calculated as

$$\begin{aligned}\tilde{\mathbf{y}}_1(0) &= \sqrt{P_2}S_2(0)\,\mathbf{h}_{12}(0) + \mathbf{n}_1(0),\\ \tilde{\mathbf{y}}_1(1) &= \sqrt{P_2}S_2(1)\,\mathbf{h}_{12}(1) + \sqrt{P_2}S_2(0)\,\mathbf{h}_{13}(1) + \mathbf{n}_1(1).\end{aligned} \tag{15}$$

By using the least square (LS) decoder, the transmitted signal can be recovered as

$$\widetilde{U}_2(1) = \arg\min_{U_k(1)} \left\|\tilde{\mathbf{y}}_1(1) - U_k(1)\,\tilde{\mathbf{y}}_1(0)\right\|. \tag{16}$$

Since $S_2(0)$ is initialized as $S_2(0) = \left[\begin{smallmatrix}1\\1\end{smallmatrix}\ \begin{smallmatrix}-1\\1\end{smallmatrix}\right]$, set $\widetilde{S}_2(0) = S_2(0) = \left[\begin{smallmatrix}1\\1\end{smallmatrix}\ \begin{smallmatrix}-1\\1\end{smallmatrix}\right]$, so $\widetilde{S}_2(1) = \widetilde{U}_2(1)\widetilde{S}_2(0)$, and then $\mathbf{h}_{13}(1)$ can be estimated as

$$\begin{aligned}\tilde{\mathbf{h}}_{13}(1) = \frac{1}{\sqrt{P_2}}&\left(\widetilde{S}_2(1)^H\widetilde{S}_2(0)\right)^{-1}\\ &\cdot\left(\widetilde{S}_2(1)^H\tilde{\mathbf{y}}_1(1) - \widetilde{S}_2(0)^H\tilde{\mathbf{y}}_1(0)\right).\end{aligned} \tag{17}$$

When $t \geqslant 2$, use $\mathbb{E}\{\tilde{\mathbf{h}}_{13}\}$ instead of $\tilde{\mathbf{h}}_{13}(t)$ to increase the accuracy with

$$\tilde{\mathbf{h}}_{13_{\text{ave}}}(t) = \frac{1}{t}\sum_{n=1}^{t}\tilde{\mathbf{h}}_{13}(t). \tag{18}$$

Then the ISI part can be removed using $\tilde{\mathbf{h}}_{13_{\text{ave}}}(t)$, let $\tilde{\mathbf{y}}_1'(t)$ denote the remaining signal, and it can be calculated as

$$\begin{aligned}\tilde{\mathbf{y}}_1'(t-1) &= \tilde{\mathbf{y}}_1(t-1) - \sqrt{P_2}S_2(t-2)\,\tilde{\mathbf{h}}_{13_{\text{ave}}}(t-1)\\ &\approx \sqrt{P_2}S_2(t-1)\,\mathbf{h}_{12}(t-1) + \mathbf{n}_1(t-1),\end{aligned} \tag{19}$$

$$\begin{aligned}\tilde{\mathbf{y}}_1'(t) &= \tilde{\mathbf{y}}_1(t) - \sqrt{P_2}S_2(t-1)\,\tilde{\mathbf{h}}_{13_{\text{ave}}}(t-1)\\ &\approx \sqrt{P_2}S_2(t)\,\mathbf{h}_{12}(t) + \mathbf{n}_1(t)\\ &= \sqrt{P_2}U_2(t)\,S_2(t-1)\,\mathbf{h}_{12}(t) + \mathbf{n}_1(t)\\ &= U_2(t)\,\tilde{\mathbf{y}}_1'(t-1) + \tilde{\mathbf{n}}_1(t),\end{aligned} \tag{20}$$

where $\tilde{\mathbf{n}}_1(t) = \mathbf{n}_1(t) - U_2(t)\mathbf{n}_1(t-1)$. The transmitted signal is then detected by LS as

$$\widetilde{U}_2(t) = \arg\min_{U_k(t)} \left\|\tilde{\mathbf{y}}_1'(t) - U_k(t)\,\tilde{\mathbf{y}}_1'(t-1)\right\|, \tag{21}$$

and then $\widetilde{S}_2(t) = \widetilde{U}_2(t)\widetilde{S}_2(t-1)$, and estimate $\mathbf{h}_{13}(t)$ again using

$$\begin{aligned}\tilde{\mathbf{h}}_{13}(t) = \frac{1}{\sqrt{P_2}}&\left(\widetilde{S}_2(t)^H\widetilde{S}_2(t-1) - \widetilde{S}_2(t-1)^H\widetilde{S}_2(t-2)\right)^{-1}\\ &\cdot\left(\widetilde{S}_2(t)^H\tilde{\mathbf{y}}_1(t-1) - \widetilde{S}_2(t-1)^H\tilde{\mathbf{y}}_1(t)\right).\end{aligned} \tag{22}$$

The detection process is then repeated as described in steps (18)~(22), which improves the accuracy of $\tilde{\mathbf{h}}_{13_{\text{ave}}}(t)$ as t increases.

3.2. Detection at Node S_2. Using the same estimation method of $\tilde{\mathbf{h}}_{11}(t)$ in node S_1, $\tilde{\mathbf{h}}_{22}$ and $\tilde{\mathbf{h}}_{23}$ here can be approximated as

$$\begin{aligned}\tilde{\mathbf{h}}_{22}(t) &= \frac{1}{2L}\frac{1}{\sqrt{P_2}}\sum_{l=1}^{L}S_2(t-l)^H\mathbf{y}_2(t-l),\\ \tilde{\mathbf{h}}_{23}(t) &= \frac{1}{2(L-1)}\frac{1}{\sqrt{P_2}}\sum_{l=1}^{L}S_2(t-1-l)^H\mathbf{y}_2(t-l).\end{aligned} \tag{23}$$

Then set $\tilde{\mathbf{y}}_2(t)$ as

$$\begin{aligned}\tilde{\mathbf{y}}_2(t) &= \mathbf{y}_2(t) - \sqrt{P_2}S_2(t)\,\tilde{\mathbf{h}}_{22}(t) - \sqrt{P_2}S_2(t-1)\,\tilde{\mathbf{h}}_{23}(t)\\ &= \sqrt{P_1}S_1(t)\,\mathbf{h}_{21}(t) + \mathbf{n}_2(t)\\ &= U_1(t)\,\tilde{\mathbf{y}}_2(t-1) + \tilde{\mathbf{n}}_2(t),\end{aligned} \tag{24}$$

where $\tilde{\mathbf{n}}_2(t) = \mathbf{n}_2(t) - U_1(t)\mathbf{n}_2(t-1)$. The transmitted signal from S_1 can be detected by LS as

$$\widetilde{U}_1(t) = \arg\min_{U_k(t)} \left\|\tilde{\mathbf{y}}_2(t) - U_k(t)\,\tilde{\mathbf{y}}_2(t-1)\right\|. \tag{25}$$

However, $\tilde{\mathbf{h}}_{22}(t)$ and $\tilde{\mathbf{h}}_{23}(t)$ estimated above are not accurate enough, which will lead to error floor in the detection. The reason is that when estimating $\mathbf{h}_{22}(t)$, $\mathbb{E}\{S_2(t)^H\mathbf{y}_2(t)\}$ includes part of $\mathbb{E}\{S_2(t)^HS_2(t-1)\mathbf{h}_{23}(t)\}$. $S_2(t)$ and $S_2(t-1)$ are not completely independent in statistical terms, so $\mathbb{E}\{S_2(t)^HS_2(t-1)\mathbf{h}_{23}(t)\}$ is not $\mathbf{0}$ while $\mathbb{E}\{S_1(t)^HS_2(t-1)\mathbf{h}_{13}(t)\} = \mathbf{0}$ for node S_1. The same problem is also existing in the estimation of $\mathbf{h}_{23}(t)$. To eliminate the inaccuracy of $\tilde{\mathbf{h}}_{22}(t)$ and $\tilde{\mathbf{h}}_{23}(t)$, a method is proposed as follows. Though $\tilde{\mathbf{h}}_{22}(t)$ is not accurate enough, it can be used. Firstly, rewrite $\tilde{\mathbf{h}}_{22}(t)$ and $\tilde{\mathbf{h}}_{23}(t)$ as $\tilde{\mathbf{h}}_{22}^{(1)}(t)$ and $\tilde{\mathbf{h}}_{23}^{(1)}(t)$. Then define $\hat{\mathbf{y}}_2(t)$ as

$$\begin{aligned}\hat{\mathbf{y}}_2(t) &= \mathbf{y}_2(t) - \sqrt{P_2}S_2(t)\,\tilde{\mathbf{h}}_{22}^{(1)}(t)\\ &= \sqrt{P_1}S_1(t)\,\mathbf{h}_{21}(t) + \sqrt{P_2}S_2(t-1)\,\mathbf{h}_{23}(t) + \mathbf{n}_2(t).\end{aligned} \tag{26}$$

Use the similar estimation method of $\mathbf{h}_{13}(t)$ to estimate $\mathbf{h}_{23}(t)$; denote the result as $\widetilde{\mathbf{h}}_{23_{\text{ave}}}^{(2)}(t)$. The only difference is that $S_2(t-1)$ is already known at node S_2, which leads to a more accurate value. Set $\widehat{\mathbf{y}}_2'(t) = \mathbf{y}_2(t) - \sqrt{P_2}S_2(t-1)\widetilde{\mathbf{h}}_{23_{\text{ave}}}^{(2)}(t)$; then $\mathbf{h}_{23}(t)$ can be reestimated as

$$\widetilde{\mathbf{h}}_{22}^{(2)}(t) = \frac{1}{2L}\frac{1}{\sqrt{P_2}}\sum_{l=1}^{L} S_2(t-l)^H \widehat{\mathbf{y}}_2'(t-l). \tag{27}$$

So, $\widetilde{\mathbf{y}}_2^{(2)}(t)$ can be calculated as

$$\widetilde{\mathbf{y}}_2^{(2)}(t) = \mathbf{y}_2(t) - \sqrt{P_2}S_2(t)\,\widetilde{\mathbf{h}}_{22}^{(2)}(t) - \sqrt{P_2}S_2(t-1)\,\widetilde{\mathbf{h}}_{23_{\text{ave}}}^{(2)}(t). \tag{28}$$

The transmitted signal can be detected by LS again as

$$\widetilde{U}_1^{(2)}(t) = \arg\min_{U_k(t)} \left\| \widetilde{\mathbf{y}}_2^{(2)}(t) - U_k(t)\,\widetilde{\mathbf{y}}_2^{(2)}(t-1) \right\|. \tag{29}$$

It is proved in the simulation results that the method of reestimating $\mathbf{h}_{22}(t)$ and $\mathbf{h}_{23}(t)$ can effectively eliminate the error floor and ensure the detection performance.

3.3. Constellation Rotation. Note that the value of $\widetilde{S}_2(t)^H\widetilde{S}_2(t-1) - \widetilde{S}_2(t-1)^H\widetilde{\mathbf{S}}_2(t-2)$ can be equal to zero, which may affect the accuracy of $\widetilde{\mathbf{h}}_{13}(t)$. This issue also exists in estimating $\mathbf{h}_{23}(t)$. To solve this problem, a rotation angle is required for the symbols modulated [21]. For BPSK constellation, the effective rotation angle is in the interval $[-\pi/2, \pi/2]$. To simplify, the rotation angle may be set as $\theta = \pi/2$. Here, we give $\mathbf{s}_2(t)$ as an example on how to achieve the constellation rotation. Set $\mathbf{s}_2(t)$ as

$$\mathbf{s}_2(t) \in \begin{cases} [\pm 1, \pm 1]^T, & t = 4m-3, 4m-2 \\ [\pm i, \pm i]^T, & t = 4m-1, 4m \end{cases} \quad (m = 1, 2, \ldots), \tag{30}$$

and it is easy to calculate that

$$S_2(t) \in \begin{cases} \left\{ \pm \begin{bmatrix} 1 & -1 \\ 1 & 1 \end{bmatrix}, \pm \begin{bmatrix} 1 & 1 \\ -1 & 1 \end{bmatrix} \right\}, & t = 4m-3, 4m-2 \\ \left\{ \pm \begin{bmatrix} i & -i \\ i & i \end{bmatrix}, \pm \begin{bmatrix} i & i \\ -i & i \end{bmatrix} \right\}, & t = 4m-1, 4m \end{cases} \quad (m = 1, 2, \ldots). \tag{31}$$

Then we can get

$$\begin{aligned} &S_2(t)^H S_2(t-1) - S_2(t-1)^H S_2(t-2) \\ &\in \left\{ \pm \begin{bmatrix} 2 \pm 2i & 0 \\ 0 & 2 \pm 2i \end{bmatrix}, \pm \begin{bmatrix} 2 & \pm 2i \\ \mp 2i & 2 \end{bmatrix}, \right. \\ &\left. \pm \begin{bmatrix} \pm 2i & 2 \\ -2 & \pm 2i \end{bmatrix}, \begin{bmatrix} 0 & 2 \pm 2i \\ -2 \mp 2i & 0 \end{bmatrix} \right\}, \end{aligned} \tag{32}$$

which is impossible to be zero. This constellation rotation scheme is also applied to $\mathbf{s}_1(t)$.

4. Performance Analysis

In this section, the Pairwise Error Probability (PEP) of the asynchronous TWRNs using DDSTC is derived. Due to the effect of imperfect synchronization, performance at the two source nodes is also asymmetric, which will be analyzed as follows, respectively. Total PEP and optimum power allocation method are also discussed in this section.

4.1. PEP of Node S_1. In Section 3, the differential detection expression at S_1 is derived as $\widetilde{\mathbf{y}}_1(t) = V(t)\widetilde{\mathbf{y}}_1(t-1) + \widetilde{\mathbf{n}}_1(t)$. Define $V_{\Delta,kj}(t) = V_k(t) - V_j(t)$ and $S_{2,(\Delta,kj)}(t) = S_{2,k}(t) - S_{2,j}(t)$. The PEP of mistaking the kth STC block by the jth STC block can be evaluated by averaging the conditional PEP over the channel statistics [12] as

$$P_{kj}^{S_1}(\gamma) = \mathbb{E}_{f_i,g_i}\left[Q\left(\sqrt{\frac{\left\| V_{\Delta,kj}(t)\,\widetilde{\mathbf{y}}_1(t-1) \right\|^2}{2\sigma_{\widetilde{\mathbf{n}}_1}^2(t)}} \right)\right], \tag{33}$$

where $\gamma = P/N_0$ is the signal-to-noise ratio (SNR), P is the total transmitted power in the TWRN, and $Q(x)$ is the Gaussian Q-function. Since it is very difficult to analyze $\widetilde{\mathbf{y}}_1(t-1)$ directly, we use $\widetilde{\mathbf{y}}_1(t-1) \approx \sqrt{P_2}S_2(t-1)\mathbf{h}_{12}(t-1)$ as in (20) instead in the following analysis. In Section 2, $f_i(t)$ and $g_i(t)$ are assumed to be constant over one frame, so $\mathbf{h}_{12}(t)$ is constant; that is, $\mathbf{h}_{12}(t) = \mathbf{h}_{12}(t-1)$. Based on (8), $S_{2,(\Delta,kj)}(t) = V_{\Delta,kj}(t)S_2(t-1)$, so $P_{kj}^{S_1}(\gamma)$ can be simplified as

$$P_{kj}^{S_1}(\gamma) \approx \mathbb{E}_{f_i,g_i}\left[Q\left(\sqrt{\frac{P_2\left\| S_{2,(\Delta,kj)}(t)\,\mathbf{h}_{12}(t) \right\|^2}{2\sigma_{\widetilde{\mathbf{n}}_1}^2(t)}} \right)\right]. \tag{34}$$

As derived in Section 2, $\mathbf{h}_{12}(t) = \beta\left[\sqrt{1-\alpha_1^2}f_1 g_1 \quad \sqrt{1-\alpha_2^2}f_2 g_2^* \right]^T$. Define $\mathbf{h}_{12}(t) = \beta F(t)\widehat{\mathbf{g}}(t)$, where $\widehat{\mathbf{g}}(t) = \left[\sqrt{1-\alpha_1^2}g_1(t) \quad \sqrt{1-\alpha_2^2}g_2^*(t) \right]^T$ and $F(t) = \text{diag}\{f_1(t), f_2(t)\}$. Then, according to [12], $P_{kj}^{S_1}(\gamma)$ can be derived as

$$P_{kj}^{S_1}(\gamma) = \frac{1}{\pi}\int_0^{\pi/2} \mathbb{E}_{f_i}\left[\prod_{i=1}^{2}\left(1 + l(\theta,t)\,\lambda_i \left| f_i(t) \right|^2 \right) \right]^{-1} d\theta, \tag{35}$$

where $l(\theta,t) = P_2|\beta|^2\sigma_g^2(1-\alpha_i^2)/8(\sum_{i=1}^2 |\beta|^2|f_i(t)|^2 + 1)N_0\sin^2\theta$, and λ_i ($i \in \{1,2\}$) denotes the singular value of $S_{2,(\Delta,kj)}(t)^H S_{2,(\Delta,kj)}(t)$. The mean of $|f_i(t)|^2$ is σ_f^2, so the term $\sum_{i=1}^2 |f_i(t)|^2$ in $l(\theta,t)$ can be approximated as $\sum_{i=1}^2 |f_i(t)|^2 \approx 2\sigma_f^2$. Hence,

$$l(\theta,t) \approx l'(\theta) = \frac{P_2|\beta|^2\sigma_g^2\left(1-\alpha_i^2\right)}{8\left(2|\beta|^2\sigma_f^2 + 1\right)N_0\sin^2\theta}. \tag{36}$$

$P_{kj}^{S_1}(\gamma)$ can then be expressed as

$$P_{kj}^{S_1}(\gamma) = \frac{1}{\pi}\int_0^{\pi/2} \mathbb{E}_{f_i}\left[\prod_{i=1}^{2}\left(1 + l'(\theta)\,\lambda_i |f_i(t)|^2\right)\right]^{-1} d\theta. \quad (37)$$

It can be observed from (37) that the influence factor of $P_{kj}^{S_1}(\gamma)$ is the same as in synchronization case except the term $(1-\alpha_i^2)$. However, $(1-\alpha_i^2)$ is a constant during a frame. So the PEP expression of node S_1 can be simplified at high SNR as

$$\begin{aligned} P_{kj}^{S_1}(\gamma) &\approx \frac{1}{2}\frac{3!!}{4!!}\prod_{i=1}^{2}\left[\left(\frac{1}{M_i}\right)\ln(M_i)\right] \\ &= \frac{3}{16}\prod_{i=1}^{2}\left[\left(\frac{1}{M_i}\right)\ln(M_i)\right], \end{aligned} \quad (38)$$

where $M_i = (P_2|\beta|^2\sigma_f^2\sigma_g^2(1-\alpha_i^2)/8(2|\beta|^2\sigma_f^2+1)N_0)\lambda_i$. Since the total transmission power is P, $P = P_1 + P_2 + 2P_R$. Denote $P_1 = \mu_1 P$, $P_2 = \mu_2 P$, and $\gamma = P/N_0$. So M_i at high SNR can be expressed as $M_i = C_{1i}\lambda_i\gamma$, where $C_{1i} = \mu_2(1-\mu_1-\mu_2)\sigma_f^2\sigma_g^2(1-\alpha_i^2)/16((1-\mu_1-\mu_2)\sigma_f^2 + \mu_1\sigma_f^2 + \mu_2\sigma_g^2)$. Thus, the simplified PEP at high SNR can be rewritten as

$$\begin{aligned} P_{kj}^{S_1}(\gamma) &= \frac{3}{16}\frac{1}{\prod_{i=1}^{2}C_{1i}\lambda_i}\gamma^{-2}\prod_{i=1}^{2}\left(\ln(C_{1i}\lambda_i) + \ln(\gamma)\right) \\ &\approx \frac{3}{16}\frac{1}{\prod_{i=1}^{2}C_{1i}\lambda_i}\gamma^{-2}[\ln(\gamma)]^2. \end{aligned} \quad (39)$$

4.2. PEP of Node S_2. Similarly to the derivation of PEP at node S_1, PEP of node S_2 can be expressed as

$$P_{kj}^{S_2}(\gamma) \approx \mathbb{E}_{f_i,g_i}\left[Q\left(\sqrt{\frac{P_1\left\|S_{1,(\Delta,kj)}(t)\,\mathbf{h}_{21}(t)\right\|^2}{2\sigma_{\tilde{\mathbf{n}}_2}^2(t)}}\right)\right], \quad (40)$$

where $\sigma_{\tilde{\mathbf{n}}_2}^2(t) = 2(\sum_{i=1}^{2}|\beta_i(t)|^2|g_i(t)|^2 + 1)N_0$ and $S_{1,(\Delta,kj)}(t) = S_{1,k}(t) - S_{1,j}(t)$. If we define $\mathbf{h}_{21}(t) = \beta G(t)\widehat{\mathbf{f}}(t)$, where $\widehat{\mathbf{f}}(t) = [f_1(t)\ \ f_2^*(t)]^T$ and $G(t) = \mathrm{diag}\{g_1(t), g_2(t)\}$, it is easy to find that the elements in $P_{kj}^{S_2}(\gamma)$ have no relationship to the imperfect synchronization coefficient α_i; that is, it is identical to the synchronization situation [12]. So $P_{kj}^{S_2}(\gamma)$ can be derived as

$$P_{kj}^{S_2}(\gamma) \approx \frac{3}{16}\frac{1}{\prod_{i=1}^{2}C_{2i}\lambda_i}\gamma^{-2}[\ln(\gamma)]^2, \quad (41)$$

where $C_{2i} = \mu_2(1-\mu_1-\mu_2)\sigma_f^2\sigma_g^2/16((1-\mu_1-\mu_2)\sigma_g^2 + \mu_1\sigma_f^2 + \mu_2\sigma_g^2)$.

4.3. Optimum Power Allocation. In order to analyze the overall performance of the system, the total PEP is considered. It can be calculated as

$$\begin{aligned} &P_{kj}^{S_1}(\gamma) + P_{kj}^{S_2}(\gamma) \\ &\quad\approx \frac{3}{16}\frac{1}{\prod_{i=1}^{2}\lambda_i}\left(\prod_{i=1}^{2}C_{1i}^{-1} + \prod_{i=1}^{2}C_{2i}^{-1}\right)\gamma^{-2}[\ln(\gamma)]^2 \\ &\quad= \frac{3}{16}\frac{1}{\prod_{i=1}^{2}\lambda_i}\left(C_{11}^{-1}C_{12}^{-1} + C_{21}^{-1}C_{22}^{-1}\right)\gamma^{-2}[\ln(\gamma)]^2. \end{aligned} \quad (42)$$

It is obvious that, to minimize the PEP at high SNR, $(C_{11}^{-1}C_{12}^{-1} + C_{21}^{-1}C_{22}^{-1})$ should be minimized. For simplification, the source nodes and the relay nodes are assumed to have the same power, which is to say $P_1 + P_2 = 2P_R = (1/2)P$; that is, $\mu_1 + \mu_2 = 1/2$; then C_{1i}, C_{2i} can be rewritten as $C_{1i} = \mu_2\sigma_f^2\sigma_g^2(1-\alpha_i^2)/32((1-\mu_2)\sigma_f^2 + \mu_2\sigma_g^2)$, $C_{2i} = (0.5-\mu_2)\sigma_f^2\sigma_g^2/32((0.5+\mu_2)\sigma_g^2 + (0.5-\mu_2)\sigma_f^2)$. Two cases are considered for further performance analysis. For case I, $\sigma_f^2 = \sigma_g^2 = \sigma^2$. For case II, $\sigma_f^2 = 10\sigma^2$, $\sigma_g^2 = \sigma^2$. In case I, $(C_{11}^{-1}C_{12}^{-1} + C_{21}^{-1}C_{22}^{-1})$ can be simplified as

$$\begin{aligned} &\left(C_{11}^{-1}C_{12}^{-1} + C_{21}^{-1}C_{22}^{-1}\right) \\ &\quad= \frac{32}{\mu_2(1-\alpha_1^2)\sigma^2}\frac{32}{\mu_2(1-\alpha_2^2)\sigma^2} + \left[\frac{32}{(0.5-\mu_2)\sigma^2}\right]^2 \\ &\quad= \frac{32^2}{\sigma^4(1-\alpha_1^2)(1-\alpha_2^2)} \\ &\qquad\times \frac{\left(2-\alpha_1^2-\alpha_2^2+\alpha_1^2\alpha_2^2\right)\mu_2^2 - \mu_2 + 0.25}{\mu_2^2(0.5-\mu_2)^2}. \end{aligned} \quad (43)$$

Denote $y(\mu_2) = ((2-\alpha_1^2-\alpha_2^2+\alpha_1^2\alpha_2^2)\mu_2^2 - \mu_2 + 0.25)/\mu_2^2(0.5-\mu_2)^2$; obviously, when $(C_{11}^{-1}C_{12}^{-1} + C_{21}^{-1}C_{22}^{-1})$ obtain the minimum value, $y(\mu_2)$ is minimum. This minimum value can be calculated by mathematical tools on computer easily, and the corresponding value of μ_2 leads to the optimum power allocation of this system. Similarly, in case II, $(C_{11}^{-1}C_{12}^{-1} + C_{21}^{-1}C_{22}^{-1})$ can be simplified as

$$\begin{aligned} &\left(C_{11}^{-1}C_{12}^{-1} + C_{21}^{-1}C_{22}^{-1}\right) \\ &\quad= \frac{16(10-9\mu_2)}{5\mu_2(1-\alpha_1^2)\sigma^2}\frac{16(10-9\mu_2)}{5\mu_2(1-\alpha_2^2)\sigma^2} + \left[\frac{16(5.5-9\mu_2)}{5(0.5-\mu_2)\sigma^2}\right]^2 \\ &\quad= \frac{256}{25\sigma^4\Phi}\left((162+\Phi)\mu_2^4 + (-261-99\Phi)\mu_2^3\right. \\ &\qquad\left. + (300.25+30.25\Phi)\mu_2^2 - 145\mu_2 + 25\right) \\ &\qquad\times\left(\mu_2^2(0.5-\mu_2)^2\right)^{-1}, \end{aligned} \quad (44)$$

where $\Phi = (1-\alpha_1^2)(1-\alpha_2^2)$. The OPA method also referred to the value of μ_2 when $(C_{11}^{-1}C_{12}^{-1} + C_{21}^{-1}C_{22}^{-1})$ is minimum.

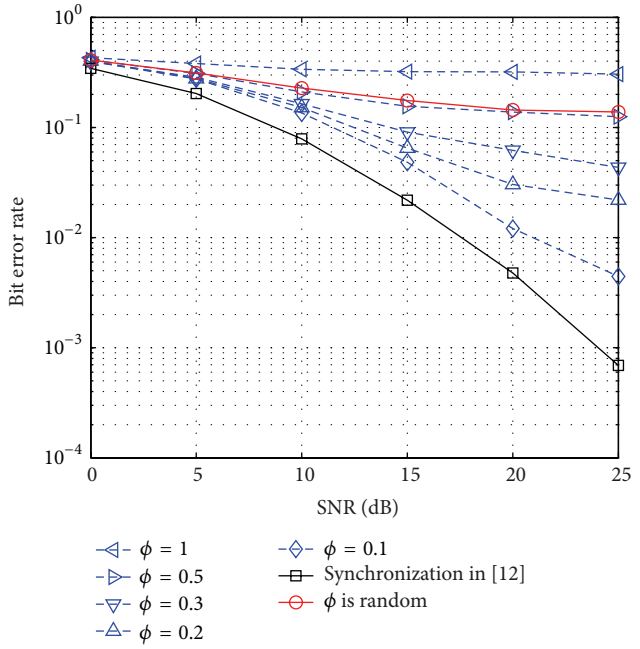

Figure 2: Effect of different imperfect synchronization coefficient ϕ.

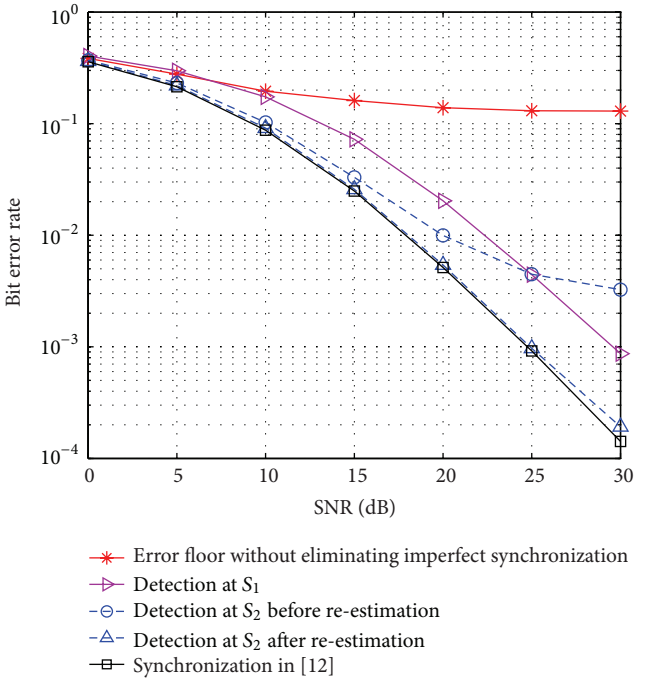

Figure 3: BER performance of detection scheme on nodes S_1 and S_2.

5. Simulation Results

In this section, simulation results of the BER performance on both sides using the proposed signal detection and the OPA scheme are presented. Rayleigh fading channel is used as the channel model in the simulations. Transmitted power of the relay nodes is assumed as $P_{R_i} = P_{1,2} = 1$, that is, equal power allocation (EPA), if not specially pointed out. BPSK modulation is used, and the frame length is $L = 100$.

Figure 2 shows the performance of TWRN under imperfect synchronization using the existing differential detection scheme in [12]. Set $\phi = \alpha/\sqrt{1-\alpha^2}$, the normalized imperfect synchronization coefficients, and take its values as 1, 0.5, 0.3, 0.2, and 0.1 for the simulations. For comparison, the performance of the TWRN under perfect synchronization is also presented [12]. It can be concluded easily that, with α increasing, the detection error floor becomes higher. But in the real system, ϕ is generated randomly since α is a random value, ranging from 0 to 1. The result is also provided in Figure 2; in this case, the error floor is almost the same as the case that $\phi = 0.5$.

Figure 3 shows the detection performance of the two source nodes using the proposed differential detection schemes for the two sides. It can be observed that the detection schemes proposed for both nodes S_1 and S_2 remove the high error floor caused by imperfect synchronization. The detection method on node S_2 eliminates the error floor at high SNR after reestimating $\mathbf{h}_{23}(t)$, providing a BER performance approaching the synchronization situation. The BER of node S_1 is 4 dB less than that of node S_2. The reason is that element $S_2(t-1)$ in the interference part is known to node S_2 but unknown to node S_1, which has been mentioned in Section 3.

In Figure 4, it shows the BER performance of the proposed differential detection and power allocation scheme. It can be observed that, in both case I and case II, the BER of node S_1 decreased while that of node S_2 increased compared to equal power allocation (EPA), and the total BER of node S_1 and node S_2 is decreased for about 1 dB. So, it is obvious that OPA can balance the asymmetric performance of the signal detection at the two sources caused by imperfect synchronization, while the performance of the whole system can also be improved.

6. Conclusion

In this paper, we have proposed a signal detection scheme for TWRN under imperfect synchronization when neither the sources nor the relays have any knowledge of CSI. Due to the effect of imperfect synchronization, detection schemes and performance are different for both sources. Simulation results indicate that the proposed algorithms on both sides perform well, with the imperfect synchronization effect greatly removed. Furthermore, we derived the simplified PEP of the TWRN and determined the optimum power allocation scheme, which improves the performance of the whole system and leads to a symmetrical detection performance for both sides even though imperfect synchronization exists.

Conflict of Interests

The authors declare that there is no conflict of interests regarding the publication of this paper.

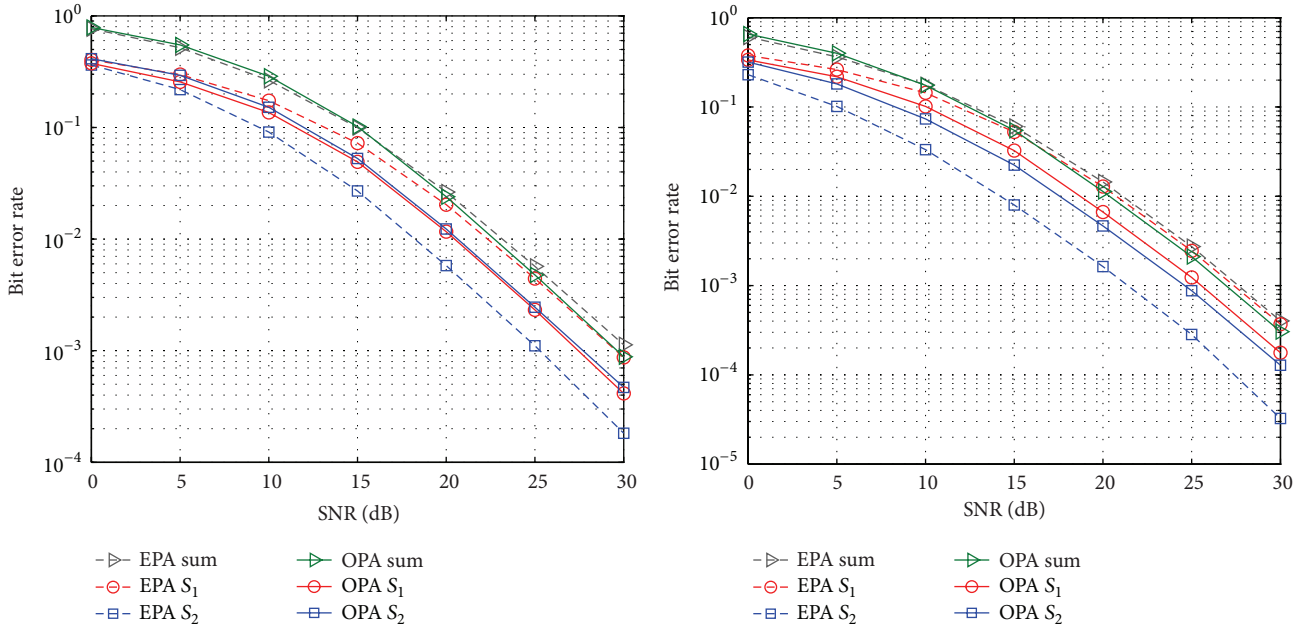

(a) Case I: $\sigma_f^2 = \sigma_g^2 = 1$

(b) Case II: $\sigma_f^2 = 10, \sigma_g^2 = 1$

FIGURE 4: BER performance of the proposed detection scheme with optimum power allocation.

Acknowledgments

This work was supported in part by Shanghai leading academic discipline project under Grant nos. S30108, 08DZ2231100, Shanghai Natural Science Foundation under Grant no. 14ZR1415100, the National Natural Science Foundation of China under Grant no. 60972055, no. 61132003, and no. 61171086, funding of Key Laboratory of Wireless Sensor Network and Communication, Shanghai Institute of Microsystem and Information Technology, funding of Shanghai Education Committee, Chinese Academy of Sciences and Shanghai Science Committee under Grant no. 12511503303, and Key Laboratory of Specialty Fiber Optics and Optical Access Networks, Shanghai University, under Grant SKLSFO2012-04.

References

[1] A. Sendonaris, E. Erkip, and B. Aazhang, "User cooperation diversity—part I: system description," *IEEE Transactions on Communications*, vol. 51, no. 11, pp. 1927–1938, 2003.

[2] A. Nosratinia, T. E. Hunter, and A. Hedayat, "Cooperative communication in wireless networks," *IEEE Communications Magazine*, vol. 42, no. 10, pp. 74–80, 2004.

[3] S. Zhang, S. Liew, and P. Lam, " Physical layer network coding," in *Proceedings of the ACM MobiCom Conference*, pp. 153–162, Los Angeles, Calif, USA, 2006.

[4] P. A. Anghel and M. Kaveh, "On the performance of distributed space-time coding systems with one and two non-regenerative relays," *IEEE Transactions on Wireless Communications*, vol. 5, no. 2, pp. 682–692, 2006.

[5] Y. Jing and B. Hassibi, "Distributed space-time coding in wireless relay networks," *IEEE Transactions on Wireless Communications*, vol. 5, no. 12, pp. 3524–3536, 2006.

[6] T. Cui, F. Gao, T. Ho, and A. Nallanathan, "Distributed space-time coding for two-way wireless relay networks," in *Proceedings of the IEEE International Conference on Communications (ICC '08)*, pp. 3888–3892, May 2008.

[7] B. M. Hochwald and W. Sweldens, "Differential unitary space-time modulation," *IEEE Transactions on Communications*, vol. 48, no. 12, pp. 2041–2052, 2000.

[8] Y. Jing and H. Jafarkhani, "Distributed differential space-time coding for wireless relay networks," *IEEE Transactions on Communications*, vol. 56, pp. 1092–1100, 2008.

[9] P. Popovski and H. Yomo, "Wireless network coding by amplify-and-forward for bi-directional traffic flows," *IEEE Communications Letters*, vol. 11, no. 1, pp. 16–18, 2007.

[10] S. Katti, S. Gollakota, and D. katabi, "Embracing wireless interference: analog network coding," in *Proceedings of the Conference on Applications, Technologies, Architectures, and Protocols for Computer Communications (ACM SIGCOMM '07)*, pp. 397–408, ACM, 2007.

[11] B. Maham, A. Hjørungnes, and G. Abreu, "Distributed GABBA space-time codes in amplify-and-forward relay networks," *IEEE Transactions on Wireless Communications*, vol. 8, no. 4, pp. 2036–2045, 2009.

[12] Q. Huo, L. Song, Y. Li, and B. Jiao, "A distributed differential space-time coding scheme with analog network coding in two-way relay networks," *IEEE Transactions on Signal Processing*, vol. 60, no. 9, pp. 4998–5004, 2012.

[13] L. Lu and S. C. Liew, "Asynchronous physical-layer network coding," *IEEE Transactions on Wireless Communications*, vol. 11, no. 2, pp. 819–831, 2012.

[14] W. Geng, T. Lv, R. Cao, and Y. Lu, "An efficient decoding algorithm based on orthogonal projection method for asynchronous physical-layer network coding," in *Proceedings of the 19th International Conference on Telecommunications (ICT '12)*, pp. 1–5, April 2012.

[15] Z. Wu, L. Liu, Y. Jin, and L. Song, "Signal detection for differential bidirectional relaying with analog network coding under imperfect synchronisation," *IEEE Communications Letters*, vol. 17, no. 6, pp. 1132–1135, 2013.

[16] F.-C. Zheng, A. G. Burr, and S. Olafsson, "Near-optimum detection for distributed space-time block coding under imperfect synchronization," *IEEE Transactions on Communications*, vol. 56, no. 11, pp. 1795–1799, 2008.

[17] C. Xu, L. Song, Z. Han, Q. Zhao, X. Wang, and B. Jiao, "Efficient resource allocation for device-to-device underlaying networks using combinatorial auction," *IEEE Journal on Selected Areas in Communications*, vol. 31, no. 9, pp. 348–358, 2013.

[18] C. Xu, L. Song, and Z. Han, *Resource Management for Device-to-Device Underlay Communication*, Springer Briefs in Computer Science, Springer, 2014.

[19] T. Cui, F. Gao, and C. Tellambura, "Differential modulation for two-way wireless communications: a perspective of differential network coding at the physical layer," *IEEE Transactions on Communications*, vol. 57, no. 10, pp. 2977–2987, 2009.

[20] B. Hassibi and B. Hochwald, "High-rate codes that are linear in space and time," *IEEE Journal on Selected Areas in Communications*, vol. 48, no. 7, pp. 1804–1824, 1804.

[21] L. Song, Y. Li, A. Huang, B. Jiao, and A. V. Vasilakos, "Differential modulation for bidirectional relaying with analog network coding," *IEEE Transactions on Signal Processing*, vol. 58, no. 7, pp. 3933–3938, 2010.